

Testing the Ampère-Maxwell law on the photon mass and Lorentz-Poincaré symmetry violation with MMS multi-spacecraft data

Alessandro D.A.M. Spallicci ^{*},^{1,2,3,4} Giuseppe Sarracino [†],⁵ Orélien Randriamboarison [‡],^{1,3,4} and José A. Helayël-Neto ^{§6}

¹Laboratoire de Physique et Chimie de l'Environnement et de l'Espace (LPC2E) UMR 7328
Université d'Orléans (UO), Centre National de la Recherche Scientifique (CNRS), Centre National d'Études Spatiales (CNES)
3A Avenue de la Recherche Scientifique, 45071 Orléans, France

²Institut Denis Poisson (IDP) UMR 7013
Université d'Orléans (UO) et Université de Tours (UT), Centre National de la Recherche Scientifique (CNRS)
Parc de Grandmont, 37200 Tours, France

³UFR Sciences et Techniques, Université d'Orléans (UO), Rue de Chartres, 45100 Orléans, France

⁴Observatoire des Sciences de l'Univers en région Centre (OSUC) UMS 3116, Université d'Orléans (UO)
1A rue de la Férollerie, 45071 Orléans, France

⁵Dipartimento di Fisica E. Pancini, Università degli Studi di Napoli, Federico II, and
Istituto Nazionale di Fisica Nucleare (INFN), Sezione di Napoli

Complesso Universitario Monte S. Angelo, Via Cinthia 9 Edificio G, 80126 Napoli, Italy

⁶Departamento de Astrofísica, Cosmologia e Interações Fundamentais (COSMO), Centro Brasileiro de Pesquisas Físicas (CBPF)
Rua Xavier Sigaud 150, 22290-180 Urca, Rio de Janeiro, RJ, Brazil

(Dated: 16 June 2022)

The photon is commonly believed being the only free massless particle. Deviations from the Ampère-Maxwell law, due to a photon mass, real for the de Broglie-Proca theory, or effective for the Lorentz-Poincaré Symmetry Violation (LSV) in the Standard-Model Extension (SME) were sought in six years of MMS satellite data. In a minority of cases, out of which 76% in modulus and 65% in Cartesian components for the highest time resolution burst data and best tetrahedron configurations in the solar wind and peripheries, deviations have been found. After currents error analysis, the minimal photon mass would be 1.74×10^{-53} kg while the minimal LSV parameter $|\vec{k}^{\text{AF}}|$ value would be $4.95 \times 10^{-11} \text{ m}^{-1}$. These values are compared with actual limits and discussed.

Non-Maxwellian electromagnetism.— Astrophysical observations are largely based on electromagnetic signals read with the Maxwellian massless and linear theory, possibly an approximation of a larger theory, as Newtonian gravity is for Einsteinian gravity in weak fields. Herein, we examine the effects of the Extended Theories of Electromagnetism (ETE) on the Ampère-Maxwell law through analysis of the currents in the Earth neighbourhood.

De Broglie first proposed a massive photon estimated below 10^{-53} kg [1], through dispersion analysis (the group velocity differs from c by a factor proportional to the inverse square of the frequency) and wrote the modified Ampère-Maxwell equations [2]. His scholar Proca wrote a Lagrangian for electrons, positrons, neutrinos and photons, asserting the masslessness of the latter two [3, 4]. The de Broglie-Proca (dBP) theory is not Lorenz gauge-invariant (a change in the potential implies a change in the field), but it satisfies Lorentz-Poincaré Symmetry (LoSy), for which measurements are independent of the orientation or velocity of the observer. Later theories gained gauge-invariance [5–7]. For renormalisation, unitarity, origin of mass and charge conservation see, e.g., [8–13]; for other discussions, see, e.g., [14–27].

Theories going beyond the Standard-Model (SM) were pro-

posed, such as the SM Extension (SME) [28, 29], based on LoSy Violation (LSV). The SME leads to an effective, gauge-invariant but anisotropic photon mass [30, 31] proportional to the LSV parameters, represented by a k_{α}^{AF} 4-vector for the odd handedness of the Charge conjugation-Parity-Time reversal (CPT) symmetry and by a $k_{\text{F}}^{\text{avp}\sigma}$ tensor when even. The k_{α}^{AF} vector from the Carroll-Field-Jackiw Lagrangian [32] always induces a mass, while the $k_{\text{F}}^{\text{avp}\sigma}$ tensor only in Super-Symmetry after photino integration [30, 31].

Born-Infeld [33, 34] and Heisenberg-Euler [35] started investigations on Non-Linear Electro-Magnetism (NLEM).

All three conceptions (dBP, SME, NLEM) lead to: a deviation from Ampère-Maxwell's law; light dispersion with a bearing on multi-messenger astronomy; a photon frequency shift *in vacuo* with a bearing on the red shift [36–38].

A photon mass damps the interaction at a distance r by a factor $e^{-r/\lambda}$, λ_{C} being the Compton reduced length. Tinier photon masses may be thus sought through large scale measurements [13]. Therefore, we analyse the Ampère-Maxwell law, through the NASA Magnetospheric Multiscale Mission (MMS) [39–41], as it has been done for the ESA Cluster satellites [42]. MMS was launched on 13 March 2015 and it is composed by four identical satellites flying in tetrahedral formation, passing through different zones of the Earth neighbourhood. The instruments on board include particle detectors and magnetometers. We use SI units and the Geocentric Solar Ecliptic (GSE) coordinate system.

Modified Ampère-Maxwell law.— The dBP equations differ from those of Maxwell in the divergence of the electric field \vec{E} and in the curl of the magnetic field \vec{B} . The latter is [2]

*email: spallicci@cnrs-orleans.fr

†email: giuseppe.sarracino@unina.it

‡email: orelie.randriamboarison@cnrs-orleans.fr

§email: helayel@cbpf.br

$$\frac{\nabla \times \vec{B}}{\mu_0} = \vec{j} + \epsilon_0 \frac{\partial \vec{E}}{\partial t} - \frac{m_\gamma^2 c^2}{\mu_0 \hbar^2} \vec{A}. \quad (1)$$

For $m_\gamma c / \hbar = 1/\lambda$, m_γ is the photon mass, c the light speed, \hbar Js the reduced Planck constant, ϵ_0 the permittivity, μ_0 the permeability, \vec{j} the current density vector, \vec{A} the vector potential.

Instead, in the SME, the Ampère-Maxwell law becomes for the CPT-odd handedness [30, 31]

$$\frac{\nabla \times \vec{B}}{\mu_0} = \vec{j} + \epsilon_0 \frac{\partial \vec{E}}{\partial t} + \frac{k_0^{\text{AF}} \vec{B}}{\mu_0} - \vec{k}^{\text{AF}} \times \frac{\vec{E}}{\mu_0 c}, \quad (2)$$

where k_0^{AF} and \vec{k}^{AF} are the time and space components of the LSV vector. If $k_0^{\text{AF}} = 0$, we established that

$$m_\gamma = \frac{\hbar |k^{\text{AF}}|}{c} x, \quad (3)$$

where x , an angular factor depending on the difference between the preferred frame and observer directions, equals unity in the photon rest frame [30].

For NLEM theories, we have set a generalised Lagrangian, encompassing the formalisms of Born-Infeld and Euler-Heisenberg [33–35], as a polynomial, function of integer powers of the field and its dual: $\mathcal{L} = \mathcal{L}(\mathcal{F}, \mathcal{G})$, where

$$\mathcal{F} = \frac{1}{2\mu_0} \left(\frac{\vec{E}^2}{c^2} - \vec{B}^2 \right) \quad \mathcal{G} = \frac{1}{\mu_0 c} \vec{E} \cdot \vec{B}.$$

The modified Ampère-Maxwell equation becomes

$$\frac{\nabla}{\mu_0} \times \left(\frac{\partial \mathcal{L}}{\partial \mathcal{F}} \vec{B} - \frac{1}{c} \frac{\partial \mathcal{L}}{\partial \mathcal{G}} \vec{E} \right) = \vec{j} + \frac{\epsilon_0}{\partial t} \left(\frac{\partial \mathcal{L}}{\partial \mathcal{F}} \vec{E} + c \frac{\partial \mathcal{L}}{\partial \mathcal{G}} \vec{B} \right). \quad (4)$$

Whether in the NLEM framework the photon acquires an effective mass is not yet settled. Equations (1,2,4) are cast as

$$\vec{j}_B = \vec{j}_P + \vec{j}_E + \vec{j}_{NM}, \quad (5)$$

where $\vec{j}_B = \nabla \times \vec{B} / \mu_0$, $\vec{j}_P = \vec{j}$, $\vec{j}_E = \epsilon_0 (\partial \vec{E} / \partial t)$, and \vec{j}_{NM} indicates the non-Maxwellian terms.

Existing upper limits. Recently, many studies, e.g., [43–51], have been conducted on Fast Radio Bursts to set upper limits through dispersion analysis [52], achieving 3.9×10^{-51} kg at 95% confidence level [50]. These limits suffer of ambiguity, since the plasma and photon time delays are indistinguishable in the measurements [53], unless working at gamma-ray frequencies [54].

A space project was proposed for improving dispersion limits [53]. The best laboratory test on Coulomb's law sets the limit at 2×10^{-50} kg [55]. In the Cluster data analysis work [42], apart from three upper limits ranging from 1.4×10^{-49} to 3.4×10^{-51} kg depending on the value of the estimated potential, there is also a critique of two results, 10^{-52} kg [56] and 2×10^{-54} kg [57]. The latter stands as the actual official upper

limit [58]. As the former, it is based entirely on Parker's model [59] and on a qualitative reasoning *ad absurdum*. Remarkably, in [56, 57] data are not presented and an error analysis is absent. Further, Eq. (4) in [57] is tested against just one single set of three data: magnetic field, ion density and particle velocity, taken from the missions Pioneer and Voyager; if the values were to vary of 50%, the limit would worsen of one order of magnitude. Despite one century of painstaking efforts, we are still dealing with estimates close to the 1923 value [1]. We consider all explorations below 10^{-51} kg being worth of a scrupulous analysis. The lowest value for any mass is dictated by Heisenberg's principle $m \geq \hbar / \Delta t c^2$, and gives 1.3×10^{-69} kg, where Δt is the supposed age of the Universe [60, 61].

For LSV, $|\vec{k}^{\text{AF}}| < 4 \times 10^{-7} \text{ m}^{-1}$ or $5 \times 10^{-4} \text{ m}^{-1}$ for laboratory tests [62], while for the astrophysical estimates $|\vec{k}^{\text{AF}}| < 5 \times 10^{-28} \text{ m}^{-1}$ [63]; $k_0^{\text{AF}} < 5 \times 10^{-10} \text{ m}^{-1}$ for laboratory tests [62] and $k_0^{\text{AF}} < 5 \times 10^{-28} \text{ m}^{-1}$ for astrophysical estimates [63]. Astrophysical estimates are close to the Heisenberg limit.

Method and data analysis.— The MMS data are contained in the Automated Multi-Dataset Analysis (AMDA) online analysis tool for heliospheric and planetary plasma [64].

AMDA provides [40, 41] the ion (electron) densities n_i (n_e), the velocities \vec{v}_i (\vec{v}_e), and the charge q . We do not take the neutrality condition for granted and compute the plasma current directly in AMDA as

$$\vec{j}_P = q(n_i \vec{v}_i - n_e \vec{v}_e). \quad (6)$$

In Cartesian components (x, y, z) , $j_P^x = q(n_i v_i^x - n_e v_e^x)$ and similarly for y, z ; the modulus is $j_P = \sqrt{(j_P^x)^2 + (j_P^y)^2 + (j_P^z)^2}$. We computed the error on j_P through propagation starting from the errors on the velocities and densities, present in AMDA [65, 66]. Later, we computed the mean of j_P for the four spacecraft, considering their errors.

For $\Delta j_P^x = q(v_i^x \Delta n_i + n_i \Delta v_i^x + v_e^x \Delta n_e + n_e \Delta v_e^x)$ and similarly for y, z , the total error is

$$\Delta j_P = \frac{1}{j_P} \left(|j_P^x| \Delta j_P^x + |j_P^y| \Delta j_P^y + |j_P^z| \Delta j_P^z \right). \quad (7)$$

AMDA provides j_B , but no information for determining its error. Therefore, we have implemented the curlmeter technique [67, 68] for computing both quantities. We consider a linear approximation of the gradient of the magnetic field measured by the four spacecraft ($\ell = 1, 2, 3, 4$). Under this assumption, \vec{j}_B is [69]

$$\vec{j}_B = \frac{1}{\mu_0} \sum_{\ell=1}^4 \vec{k}_\ell \times \vec{B}_\ell, \quad (8)$$

where \vec{k}_ℓ are the reciprocal vectors of the tetrahedron, defined by $(\vec{r}_{ij} = \vec{r}_j - \vec{r}_i)$, where i and j refer to the spacecraft positions)

$$\vec{k}_1 = \frac{\vec{r}_{23} \times \vec{r}_{24}}{\vec{r}_{21} \cdot (\vec{r}_{23} \times \vec{r}_{24})}, \quad \vec{k}_2 = \frac{\vec{r}_{31} \times \vec{r}_{34}}{\vec{r}_{32} \cdot (\vec{r}_{31} \times \vec{r}_{34})},$$

$$\vec{k}_3 = \frac{\vec{r}_{24} \times \vec{r}_{21}}{\vec{r}_{23} \cdot (\vec{r}_{24} \times \vec{r}_{21})}, \quad \vec{k}_4 = \frac{\vec{r}_{32} \times \vec{r}_{31}}{\vec{r}_{34} \cdot (\vec{r}_{32} \times \vec{r}_{31})}.$$

\vec{j}_B from AMDA compares satisfactorily with our computations. The errors on \vec{j}_B depend on the uncertainties of the magnetic field and on the separations between the spacecraft. For the former, we consider a constant value $\Delta B = 0.1 \times 10^{-9}$ T for each component of the magnetic field [70], while for the latter we consider a relative error equal to 1% of the separation distance [71]. Finally, the error on the q component for a single spacecraft reads as

$$\Delta j_{\ell B}^q = (|k_{\ell}^r| + |k_{\ell}^s|)\Delta B + |B_{\ell}^r|\Delta k_{\ell}^s + |B_{\ell}^s|\Delta k_{\ell}^r, \quad (9)$$

r, s being the other components. The final error on the q^{th} component of \vec{j}_B is

$$\Delta j_B^q = \sum_{\ell=1}^4 \Delta j_{\ell B}^q. \quad (10)$$

We downloaded the data sampling at 1 s. Since the instruments were polled at a higher rate of tens of milliseconds [72, 73], we have verified that AMDA delivers the mean of the values belonging to our sampling time. Therefore, the high frequency contributions from \vec{j}_P are cut off, allowing the comparison with \vec{j}_B , typically laying at low frequencies. We have spanned almost six years of measurements, from November 2015 to September 2021. We picked only "burst mode" data [39], which are the data of the highest time resolution collected by MMS. Within this data set, we selected the time intervals i) in which both \vec{j}_B and \vec{j}_P are available, ii) and where the four \vec{j}_P currents, measured by each spacecraft - including their errors - overlap. This eases the comparison with \vec{j}_B , supposedly uniform in the tetrahedron. We have analysed approximately 3.8×10^6 data points, for each of which we have collected 30 physical quantities for further processing.

We have verified that \vec{j}_E is several orders of magnitude smaller than the curl, particle currents and their difference. We thus compared, at each second, \vec{j}_B with \vec{j}_P , Eq. (5). We label the comparison "inconsistency" if the two currents are not overlapping considering their errors. We attribute this gap to a non-Maxwellian current \vec{j}_{nM} , Eq. (5). Instead a "consistency" occurs when the two current bands overlap. Therein, we determine an upper limit to \vec{j}_{nM} , as the smallest amount to add (subtract) to (from) one of the two currents to get an inconsistency case, Fig. 1. In short, the procedure is

$$|\vec{j}_{\rho}| - \Delta|\vec{j}_{\rho}| - (|\vec{j}_{\epsilon}| + \Delta|\vec{j}_{\epsilon}|) \stackrel{\text{gap}}{\underset{\text{overlap}}{\geq}} 0, \quad (11)$$

where $\rho, \epsilon = B, P$ depending on whether $|\vec{j}_{\rho}| - \Delta|\vec{j}_{\rho}|$ is larger or smaller than $|\vec{j}_{\epsilon}| + \Delta|\vec{j}_{\epsilon}|$.

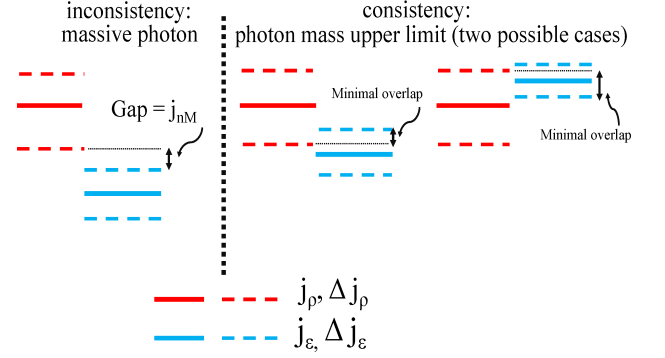


FIG. 1: The red (black) and blue (grey) lines represent the currents, and, if dotted, the error bounds. On the left, the case of inconsistency, where the gap implies $\vec{j}_{nM} \neq 0$. On the right, the case of consistency, for which moving upward or downward one of the two bands, we would fall in the inconsistency case, finding just an upper limit for \vec{j}_{nM} . This computation has been carried out for the modulus and for each component.

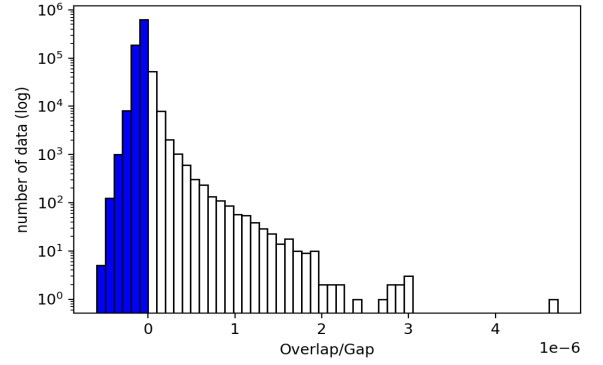


FIG. 2: Histogram of Eq. (11) for burst data. Most values are negative, blue (gray) bars, on the left of and close to zero. The positive values, white bars, on the right of zero, corresponding to the inconsistencies, range from $1.1 \times 10^{-12} \text{ Am}^{-2}$ to $4.7 \times 10^{-6} \text{ Am}^{-2}$.

This analysis has been carried for the modulus and for the Cartesian components. In the latter case, an inconsistency is declared if a gap emerges from at least one of the three axis.

Scrutinising the entire data set, we find 2% of inconsistencies for the modulus and 5.2% in Cartesian components; indeed, it may occur that the sum of the currents in absolute values is zero, but their vectorial sum is not, Eq. (5). These small percentages have not to be interpreted straightforwardly as an outcome of a foundational test, but rather as the consequence of a mission crossing mostly turbulent regions of magnetic reconnection and deploying burst modes for 86% outside the region where the majority of inconsistencies are found, Tab. 1. The analysis of Eq. (11) is shown in Fig. 2.

For the application of the curlmeter technique, the shape of the tetrahedron matters. Since this technique is sensible to the relative separations between the spacecraft [74], we select similar and quasi-optimal configurations. Referring to a

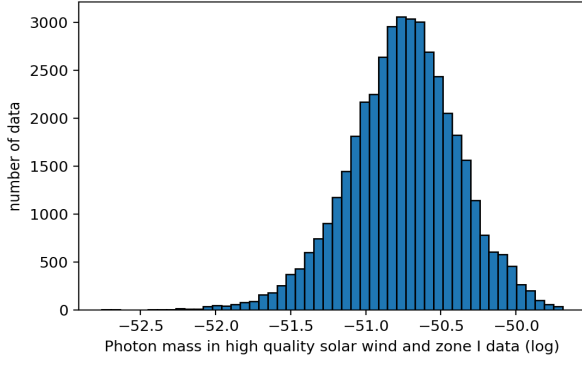


FIG. 3: For the solar wind and zone I regions burst data and $Q > 0.7$, the histogram of the photon mass derived from the inconsistencies. The minimum value is 1.74×10^{-53} kg, while the mean is 2.48×10^{-51} kg.

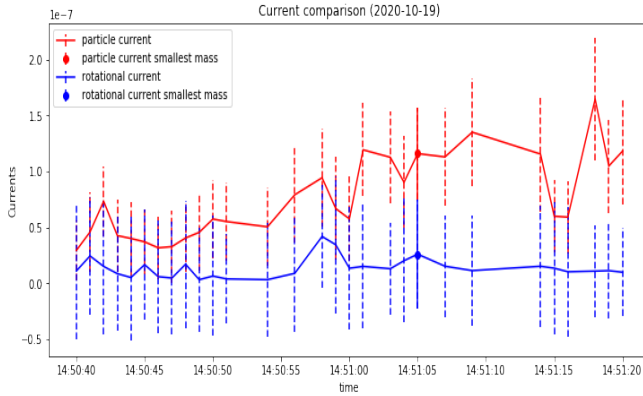


FIG. 4: The smallest photon mass, see the spots, occurs on 19 October 2020, at 14h 51m 05s, in the zone I burst data and $Q = 0.821$. The particle current $j_P = (1.16 \pm 0.41) \times 10^{-7}$ Am⁻², and the rotational current $j_B = (2.61 \pm 4.91) \times 10^{-8}$ Am⁻² produced a difference of 7.40×10^{-12} Am⁻². This difference is not visible on the vertical axis carrying units which are five orders of magnitude larger. The vertical dotted lines are the errors. The potential of 3.78×10^3 Tm⁻¹ leads to a mass of 1.74×10^{-53} kg, Eq. (12), and thereby $|\vec{k}^{AF}| = 4.95 \times 10^{-11}$ m⁻¹, Eq. (3).

regular tetrahedron, we employ the quality factor [39] on the volume $Q = V_a/V_r$, where V_a is the actual volume of the tetrahedron in a given moment, while V_r is the volume of the regular tetrahedron having as side the average of the separations between the spacecraft. We have computed Q for all our data points and set $Q > 0.7$ as threshold. By doing so, the percentages of inconsistencies slightly increase to 2.2% for the modulus and slightly decrease to 4.8% for the components.

We have localised burst data for associating inconsistencies to different physical regions and to more turbulent or quiet local plasma conditions. After examination of the constraints in [75], we opted for computing the ram p_R , magnetic p_M and thermal p_T pressures at each data point. If $p_R > 10 \max(p_M, p_T)$, we identify the region as solar wind; if $0.3 \min(p_M, p_T) < p_R < 4 \max(p_M, p_T)$, as magnetosheath; if $10 p_R < p_M$, as magnetosphere. The region of undetermined

Results	Solar Wind	Zone I	Magnetosheath	Zone II	Magnetosphere
Gaps (M)	24376	18097	10669	2203	571
Overlaps (M)	92190	261103	1033981	356592	707595
Gaps (C)	34813	43034	35422	5421	1160
Overlaps (C)	81753	236166	1009228	353374	707006
Data by region/total data	4.5%	9.5%	42.9%	14.1%	29%
Gaps by region/total gaps (M)	39%	31.1%	24%	4.5%	1.4%
Gaps/total data by region (M)	21%	6.4%	1.0%	0.6%	0.1%
Gaps/total data by region (C)	29.9%	15.3%	3.3%	1.5%	0.2%

TABLE I: Results in modulus (M) and components (C) on gaps (inconsistencies) and overlaps (consistencies) for burst data and $Q > 0.7$, analysed by region, in number and percentages.

data points between the solar wind and the magnetosheath is named Zone I, whereas between the magnetosheath and magnetosphere, Zone II, Tab. 1. For the gaps (solar wind + zone I), 76% (42473/55916) in modulus and 65% (77847/119850) by components lay in 14% of the total data.

Reliability of the analysis.— We judge the computation of j_P in the solar wind enough reliable to claim inconsistencies for the following: A) we have observed the absence of correlations between inconsistencies and particle densities; B) in the solar wind and zone I inconsistencies, the electron density has a mean of 22.96 cm^{-3} and median of 11.88 cm^{-3} ; the ion density has a mean of 22.85 cm^{-3} and median of 12.1 cm^{-3} ; only in 13.6% and 8.6% of cases the electron and ion densities, respectively, are smaller than 5 cm^{-3} ; these values appear sufficient for an adequate measurement of j_P . For the inconsistencies in all regions, we add that C) j_P is larger than j_B in 95.6% of the cases; were the errors in AMDA representative of statistical errors, but not fully of secular and calibration errors, the following cases may arise: C-i) j_P derived by AMDA is underestimated; this case would not matter, had we the 'real' j_P , its difference with j_B would increase and the gap would be deeper; C-ii) j_P is overestimated; this case may lead to: C-ii-a) tinier differences between the two currents and thereby to a smaller photon mass, for a given potential (a positive result for our study); or C-ii-b) cancel inconsistencies, but statistically compensated by the C-i) and C-ii-a) cases; D) we derive a single j_P by averaging the currents of the four spacecraft, only when the four error bands overlap; by this procedure we avoid a part of the calibration errors. Finally, we are more interested in pointing the existence of differences between currents than evaluate exactly each current.

The potential.— The current deviations are strictly an outcome of experimental data, but an estimate of the potential is mandatory to qualify the photon mass or simply state an upper limit, Eq. (1). We focus on the solar wind and zone I, where most inconsistencies emerge, and use the analytical computation of the vector potential [76] at each data point through the Parker model. A direct proportionality emerges between $|\vec{B}|$ and $|\vec{A}|$, expressed by $A = \sqrt{11/6}BR$, where R is 1 AU.

Discussion, conclusions, perspectives.— We finally assess the mass of the photon, in the gap cases, or alternatively its upper limit, in the overlap cases, Eq. (12) and estimate the LSV parameter $|\vec{k}^{AF}|$, Eq. (3). The mass values for the high quality geometrical factor are shown in Fig. 3

$$m_\gamma = \frac{\hbar \sqrt{\mu_0}}{c} \sqrt{\frac{|\vec{j}_{nM}|}{|\vec{A}|}} \text{ kg} . \quad (12)$$

The minimal value of the photon mass is 1.74×10^{-53} kg, while the mean is 2.48×10^{-51} kg, corresponding to $|\vec{k}^{\text{AF}}| = 4.95 \times 10^{-11} \text{ m}^{-1}$ and $|\vec{k}^{\text{AF}}| = 7.06 \times 10^{-9} \text{ m}^{-1}$, respectively. The mean value of the upper limit distribution is 2.21×10^{-51} kg and $|\vec{k}^{\text{AF}}| = 6.27 \times 10^{-9} \text{ m}^{-1}$. The mean value of the upper limit distribution is comparable to the mean value of the photon mass distribution. This is due to our definition of upper limit that involves the minimal displacement, upward or downward, of the current bands, Fig. 1.

In a minority of cases, a non-zero photon mass cannot be ruled out by our analysis due to the inconsistencies at some data points between j_P and j_B having considered their errors, e.g., Fig. 4. The deviations from the Ampère-Maxwell law may occur when the errors on the currents are relatively small. Furthermore, there are not stringent *experimental* constraints to definitively rule out a photon mass at 10^{-53} level (many published limits are defined speculative in [13]).

Although we find a massive photon at times, we do not intend to claim it as the final result. We are dealing with a minority of cases in six years of data and we can't exclude possible mismatches between currents, even after instrument calibration and analysis of systematic effects on MMS [39, 65, 66, 72, 73], as the intrinsic charge [77]. The instrumentation on MMS enables regular crosscalibration and validation of the Field Plasma Investigation (FPI) data, reducing systematic errors to within a few percent and providing suitable accuracy to calculate current density directly from particle observations [66]. For the Digital Flux Gate (DFG) and the Analogue Flux Gate (AFG) magnetometers, the ground calibration is refined in space to ensure all eight magnetometers are precisely inter-calibrated [73].

The determination of the nature of the deviations necessitates to explore current differences well below 10^{-12} Am^{-2} , Eq. (12), ideally four orders of magnitude, to reach the 10^{-55} kg area. While this is ambitious, it paves the way to new and far reaching, combined explorations in plasma and fundamental physics, which are usually separated domains of research. Since the curlmeter method does not allow to observe current densities smaller than the tetrahedron scale, a constellation of more than four spacecraft targeting the solar wind is desirable.

Acknowledgements.— The *Centre National des Études Spatiales* (CNES) and the *Federation Calcul Scientifique et Modélisation Orléans Tours* (CaSciModOT) for missions and the student internships of S. Dahani and A. Gauthier are thanked. Discussions with G. Chanteur and H. Breuillard (Paris), V. Génot (Toulouse), D. Gershman (NASA), B. Lavraud (Bordeaux), and the colleagues T. Dudok de Wit, P. Henri, V. Krasnoselskikh, J.-L. Pinçon (Orléans) are acknowledged. GS thanks the hospitality of LPC2E, the support by the *Istituto Nazionale di Fisica Nucleare, Sez. di Napoli, Iniziativa Specifica QGSKY* and the Erasmus+ programme.

- [1] L. de Broglie, *Comptes Rendus Hebd. Séances Acad. Sci. Paris* **177**, 507 (1923).
- [2] L. de Broglie, *Nouvelles Recherches sur la Lumière*, vol. 411 of *Actualités Scientifiques et Industrielles* (Hermann & C^{ie}, Paris, 1936).
- [3] A. Proca, *J. Phys. et Radium* **7**, 347 (1936).
- [4] A. Proca, *J. Phys. et Radium* **8**, 23 (1937).
- [5] F. Bopp, *Ann. Phys. (Leipzig)* **430**, 345 (1940).
- [6] B. Podolsky, *Phys. Rev.* **62**, 68 (1942).
- [7] E. C. G. Stueckelberg, *Helv. Phys. Acta* **30**, 209 (1957).
- [8] D. G. Boulware, *Ann. Phys.* **56**, 140 (1970).
- [9] E. Guendelman, *Phys. Rev. Lett.* **43**, 543 (1979).
- [10] S. Nussinov, *Phys. Rev. Lett.* **59**, 2401 (1987).
- [11] E. Adelberger, G. Dvali, and A. Gruzinov, *Phys. Rev. Lett.* **98**, 010402 (2007), arXiv:hep-ph/0101087.
- [12] C. Itzykson and J.-B. Zuber, *Quantum Field Theory* (Dover Publications, Mineola, 2012).
- [13] A. Scharff Goldhaber and M. M. Nieto, *Rev. Mod. Phys.* **82**, 939 (2010), arXiv:0809.1003 [hep-ph].
- [14] R. R. Cuzinatto, E. M. de Moraes, L. G. Medeiros, C. Naldoni de Souza, and B. M. Pimentel, *Europhys. Lett.* **118**, 19001 (2017), arXiv:1611.00877 [astro-ph.CO].
- [15] R. Casana, M. M. Ferreira Jr., L. Lisboa-Santos, F. E. P. dos Santos, and M. Schreck, *Phys. Rev. D* **97**, 115043 (2018), arXiv:1802.07890 [hep-th].
- [16] N. Craig and I. Garcia Garcia, *J. High Energ. Phys.* **11**, 067 (2018), arXiv:1810.05647 [hep-th].
- [17] J. Alfaro and A. Soto, *Phys. Rev. D* **100**, 055029 (2019), arXiv:1901.08011 [hep-th].
- [18] J. C. C. Felipe, H. G. Fargnoli, A. P. Baeta Scarpelli, and L. C. T. Brito, *Int. J. Mod. Phys. A* **34**, 1950139 (2019), arXiv:1807.00904 [hep-th].
- [19] M. M. Ferreira Jr., L. Lisboa-Santos, R. V. Maluf, and M. Schreck, *Phys. Rev. D* **100**, 055036 (2019), arXiv:1903.12507 [hep-th].
- [20] M. Reece, *J. High En. Phys.* **7**, 181 (2019), arXiv:1808.09966 [hep-th].
- [21] J. A. A. S. Reis, M. M. Ferreira Jr., and M. Schreck, *Phys. Rev. D* **100**, 095026 (2019), arXiv:1905.04401 [hep-th].
- [22] M. M. Ferreira Jr., J. A. Helayël-Neto, C. M. Reyes, M. Schreck, and P. D. S. Silva, *Phys. Lett. B* **804**, 135379 (2020), arXiv:2001.04706 [hep-th].
- [23] T. Srivastava and A. C. Nayak, *Eur. Phys. J. Plus* **135**, 679 (2020).
- [24] A. A. Araújo Filho and R. V. Maluf, *Braz. J. Phys.* **51**, 820 (2021), arXiv:2003.02380 [hep-th].
- [25] A. Caputo, S. J. Witte, D. Blas, and P. Pani, *Phys. Rev. D* **104**, 043006 (2021), arXiv:2102.11280 [hep-ph].
- [26] P. D. S. Silva, L. Lisboa-Santos, M. M. Ferreira Jr., and M. Schreck, *Phys. Rev. D* **104**, 116023 (2021), arXiv:2109.04659 [hep-th].
- [27] B. A. Marques, A. P. Baeta Scarpelli, J. C. C. Felipe, and L. C. T. Brito, *Adv. High En. Phys.* **69**, 7396078 (2022), arXiv:2105.13759 [hep-th].
- [28] D. Colladay and V. A. Kostelecký, *Phys. Rev. D* **55**, 6760 (1997), arXiv:hep-ph/9703464.
- [29] D. Colladay and V. A. Kostelecký, *Phys. Rev. D* **58**, 116002 (1998), arXiv:hep-ph/9809521.
- [30] L. Bonetti, L. R. dos Santos Filho, J. A. Helayël-Neto, and A. D. A. M. Spallicci, *Phys. Lett. B* **764**, 203 (2017), arXiv:1607.08786 [hep-ph].

- [31] L. Bonetti, L. R. dos Santos Filho, J. A. Helayël-Neto, and A. D. A. M. Spallicci, *Eur. Phys. J. C* **78**, 811 (2018), arXiv:1709.04995 [hep-th].
- [32] S. M. Carroll, G. B. Field, and R. Jackiw, *Phys. Rev. D* **41**, 1231 (1990).
- [33] M. Born and L. Infeld, *Proc. R. Soc. London A* **144**, 425 (1934).
- [34] M. Born and L. Infeld, *Proc. R. Soc. London A* **150**, 141 (1935).
- [35] W. Heisenberg and H. Euler, *Zeitschr. Phys.* **98**, 714 (1936).
- [36] J. A. Helayël-Neto and A. D. A. M. Spallicci, *Eur. Phys. J. C* **79**, 590 (2019), arXiv:1904.11035 [hep-ph].
- [37] A. D. A. M. Spallicci, J. A. Helayël-Neto, M. López-Corredoira, and S. Capozziello, *Eur. Phys. J. C* **81**, 4 (2021), arXiv:2011.12608 [astro-ph.CO].
- [38] A. D. A. M. Spallicci, G. Sarracino, and S. Capozziello, *Eur. Phys. J. Plus* **137**, 253 (2022), arXiv:2202.02731 [astro-ph.CO].
- [39] S. A. Fuselier, W. S. Lewis, C. Schiff, R. Ergun, J. L. Burch, S. M. Petriner, and K. J. Trattner, *Space Sci. Rev.* **199**, 77 (2016).
- [40] URL <https://mms.gsfc.nasa.gov/index.html>.
- [41] URL <https://lasp.colorado.edu/mms/sdc/public/>.
- [42] A. Retinò, A. D. A. M. Spallicci, and A. Vaivads, *Astropart. Phys.* **82**, 49 (2016), arXiv:1302.6168 [hep-ph].
- [43] L. Bonetti, J. Ellis, N. E. Mavromatos, A. S. Sakharov, E. K. Sarkisian-Grinbaum, and A. D. A. M. Spallicci, *Phys. Lett. B* **757**, 548 (2016), arXiv:1602.09135 [astro-ph.HE].
- [44] L. Bonetti, J. Ellis, N. E. Mavromatos, A. S. Sakharov, E. K. Sarkisian-Grinbaum, and A. D. A. M. Spallicci, *Phys. Lett. B* **768**, 326 (2017), arXiv:1701.03097 [astro-ph.HE].
- [45] J.-J. Wei, E.-K. Zhang, S.-B. Zhang, and X.-F. Wu, *Res. Astron. Astrophys.* **17**, 13 (2017), arXiv:1608.07675 [astro-ph.HE].
- [46] Y.-P. Yang and B. Zhang, *Astrophys. J.* **842**, 23 (2017), arXiv:1701.03034 [astro-ph.HE].
- [47] J.-J. Wei and X.-F. Wu, *J. Cosm. Astropart. Phys.* **7**, 045 (2018), arXiv:1803.07298 [astro-ph.HE].
- [48] N. Xing, H. Gao, J.-J. Wei, Z. Li, W. Wang, B. Zhang, X. Wu, and P. Mészáros, *Astrophys. J. Lett.* **882**, L13 (2019), arXiv:1907.00583 [astro-ph.HE].
- [49] J.-J. Wei and X.-F. Wu, *Res. Astron. Astrophys* **20**, 206 (2020), arXiv:2006.09680 [astro-ph.HE].
- [50] H. Wang, X. Miao, and L. Shao, *Phys. Lett. B* **820**, 136596 (2021), arXiv:2103.15299 [astro-ph.HE].
- [51] J.-J. Wei and X.-F. Wu, *Front. Phys.* **16**, 44300 (2021), arXiv:2102.03724 [astro-ph.HE].
- [52] L. de Broglie, *Recherches sur la théorie des quanta* (Masson & C^{ie}, Paris, 1924), Doctorate thesis (Dir. P. Langevin) Université de Paris, Sorbonne.
- [53] M. J. Bentum, L. Bonetti, and A. D. A. M. Spallicci, *Adv. Space Res.* **59**, 736 (2017), arXiv:1607.08820 [astro-ph.IM].
- [54] D. J. Bartlett, H. Desmond, P. G. Ferreira, and J. Jasche, *Phys. Rev. D* **104**, 103516 (2021), arXiv:2109.07850 [gr-qc].
- [55] E. R. Williams, J. E. Faller, and H. A. Hill, *Phys. Rev. Lett.* **26**, 721 (1971).
- [56] D. D. Ryutov, *Plasma Phys. Contr. Fus.* **39**, A73 (1997).
- [57] D. D. Ryutov, *Plasma Phys. Contr. Fus.* **49**, B429 (2007).
- [58] P. A. Zyla and the Particle Data Group, *Progr. Theor. Exp. Phys.* p. 083C01 (2020).
- [59] E. N. Parker, *Astrophys. J.* **128**, 664 (1958).
- [60] S. Capozziello, M. Benetti, and A. D. A. M. Spallicci, *Found. Phys.* **50**, 893 (2020), arXiv:2007.00462 [gr-qc].
- [61] A. D. A. M. Spallicci, M. Benetti, and S. Capozziello, *Found. Phys.* **52**, 23 (2022), arXiv:2112.07359 [physics.gen-ph].
- [62] Y. M. P. Gomes and P. C. Malta, *Phys. Rev. D* **94**, 025031 (2016), arXiv:1604.01102 [hep-ph].
- [63] V. A. Kostelecký and N. Russell, *Rev. Mod. Phys.* **83**, 11 (2011), arXiv:0801.0287 [hep-ph].
- [64] V. Génot, E. Budnik, C. Jacquaya, M. Bouchemit, B. Renard, N. Dufourg, N. André, B. Cecconi, F. Pitout, B. Lavraud, et al., *Plan. Space Sci.* **201**, 105214 (2021).
- [65] D. J. Gershman, J. C. Dorelli, A. F.-Viñas, and C. J. Pollock, *J. Geophys. Res. Space Phys.* **120**, 6633 (2015).
- [66] D. J. Gershman, J. C. Dorelli, L. A. Avano, U. Gliese, C. Schiff, D. E. Da Silva, W. R. Paterson, B. I. Giles, and C. J. Pollock, *J. Geophys. Res. Space Phys.* **124**, 10345 (2019).
- [67] M. W. Dunlop, D. J. Southwood, K.-H. Glassmeier, and F. M. Neubauer, *Adv. Space Res.* **8**, 273 (1988).
- [68] M. W. Dunlop, A. Balogh, K.-H. Glassmeier, and P. Robert, *J. Geophys. Res. (Space Physics)* **107**, 1384 (2002).
- [69] G. Chanteur and F. Mottez, in *Spatio-Temporal Analysis for Resolving plasma Turbulence (START)* (European Space Agency, Noordwijk, 1993), vol. ESA WPP-47, p. 341, 31 January-5 February 1993 Aussois.
- [70] R. B. Torbert, C. T. Russell, W. Magnes, R. E. Ergun, P. Lindqvist, O. LeContel, H. Vaith, J. Macri, S. Myers, D. Rau, et al., *Space Sci. Rev.* **199**, 105 (2016).
- [71] D. Kelbel, T. Lee, A. Long, R. Carpenter, and C. Gramling (2003), <https://ntrs.nasa.gov/citations/20040084078>.
- [72] C. Pollock, T. Moore, A. Jacques, J. Burch, U. Gliese, Y. Saito, T. Omoto, L. Avano, A. Barrie, V. Coffey, et al., *Space Sci. Rev.* **199**, 331 (2016).
- [73] C. T. Russell, B. J. Anderson, W. Baumjohann, K. R. Bromund, D. Dearborn, D. Fischer, G. Le, H. K. Leinweber, D. Leneman, W. Magnes, et al., *Space Sci. Rev.* **199**, 189 (2016).
- [74] M. W. Dunlop, S. Haaland, X. Dong, H. Middleton, C. P. Escoubet, Y. Yang, Q. Zhang, J. Shi, and C. T. Russell, in *Electric currents in geospace and beyond*, edited by A. Keiling, O. Marghitu, and M. Wheatland (John Wiley & Sons, Hoboken, 2018), vol. 235 of *Geophysical Monograph Series*, chap. Multipoint analysis of electric currents in geospace using the curlometer technique, p. 67, ISBN 9781119324492.
- [75] L. Rezeau and G. Belmont, *Réflexions de la physique* **59**, 20 (2018).
- [76] J. W. Bieber, P. A. Evenson, and W. H. Matthaeus, *Astrophys. J.* **315**, 700 (1987).
- [77] A. C. Barrie, F. Cipriani, C. P. Escoubet, S. Toledo-Redondo, R. Nakamura, K. Torkar, Z. Sternovsky, S. Elkington, D. Gershman, B. Giles, et al., *Phys. Plasmas* **26**, 103504 (2019).